

Anomalous diffusion in aqueous solutions of gelatin

S. Z. Ren, W. F. Shi,* W. B. Zhang,[†] and C. M. Sorensen

Department of Physics, Kansas State University, Manhattan, Kansas 66506

(Received 1 November 1990; revised manuscript received 25 September 1991)

Dynamic-light-scattering experiments on semidilute aqueous solutions of gelatin indicate three relaxation processes: an exponential for times less than $\sim 50 \mu\text{sec}$ followed by a power law at intermediate time and then a stretched exponential at long time. The characteristic time of the stretched exponential diverges as the system evolves to a gel. The latter two relaxations can be explained in terms of an anomalous diffusion mechanism where the mean-square displacement behaves as $\langle R^2 \rangle \sim \ln t$ at intermediate time and $\langle R^2 \rangle \sim t^\beta$ with $\beta < 1$ at late time. Length scales derivable from these diffusion mechanisms obey scaling, and it is proposed that β is related to the fracton density-of-states exponent and the fractal dimension of the gelatin molecules.

PACS number(s): 82.70.Gg, 05.40.+j, 61.41.+e

I. INTRODUCTION

Polymer solution dynamics in the dilute to semidilute regime is currently an area of active interest [1,2]. In the semidilute regime polymer overlap leading to topological constraints on the polymer molecule motion strongly affects the dynamics of this system and a wealth of complex phenomena have been observed. The problem of what happens when the individual molecules can bind together to form a gel begins in the semidilute solution and would seem to add to the complexity of phenomena that may occur. In this paper we present a dynamic-light-scattering study of aqueous solutions of gelatin, a biopolymer, in the semidilute regime and study the evolution from sol to gel.

Dynamic light scattering (DLS) has served as a useful probe for the molecular relaxation modes of polymer solutions. Early DLS results showed that exponential relaxations in the dilute regime became very nonexponential in the semidilute regime [3,4]. Amis and co-workers [5–7] were the first to show that this nonexponentiality was due to two modes of relaxation. In their study of aqueous gelatin solutions [5] they found two exponential modes, both q^2 dependent, where q is the scattering wave vector. The fast mode was inversely dependent on the solvent viscosity and was ascribed to cooperative diffusion related to segmental motion of the polymer chain. The slow mode was inversely proportional to the solution viscosity and hence was thought to represent motion of the polymer as a whole, hence self-diffusion. Later forced Rayleigh-scattering experiments have brought this latter assignment into question [8]. After the solution had set to a gel, the slow mode was gone, leaving only the fast mode. Earlier, Tanaka, Hocker, and Benedek [9,10] had studied DLS from set gels and found exponential decays related to the longitudinal osmotic modulus. Thus the concept was born that the solution fast mode could be also thought of as an incipient gel mode.

Since then, a number of studies have indicated the presence of two major modes of decay in semidilute poly-

mer solutions [11–18]. The fast mode is always exponential and q^2 dependent. No consensus seems to exist for the slow-mode behavior and a variety of results have been found. Typically, it is observed as nonexponential due to a broad distribution of relaxations and not q dependent. This distribution of relaxations has not been quantified and often other q dependencies are seen [5,11,12,17]. In gelled solutions the slow mode is gone leaving only the fast mode.

The sol-to-gel transition has also elicited considerable interest in the recent past due mostly to its possible description by percolation theory [19,20]. Only a few efforts, however, have applied DLS to study the evolution of sol to gel. Adam *et al.* [21] studied chemically crosslinked polyurethane by diluting samples from the reaction bath as the system gelled. DLS showed an initial exponential decay followed by a stretched exponential with width parameter β (see below) that declined with concentration until the mode was better described by a power law in time. Martin, Wilcoxon, and Odinek [22,23] used DLS to watch the sol-to-gel evolution in a system of colloidal silica particles. Once again an initial exponential was observed followed by a power law which was cut off by a stretched exponential. The characteristic time of the stretched exponential diverged to infinity as the system set to a gel.

In this work we have used DLS to study aqueous gelatin solutions over a broad range of concentrations from dilute to semidilute at temperatures above the gel transition temperature, T_{gel} , so the solution would not gel. In this regime we observe three decays: a fast exponential, an intermediate power law, and a long-time stretched exponential. We then temperature quenched our systems to temperatures less than T_{gel} and watched the modes evolve as the system gelled. Qualitatively our results bear resemblance to earlier work on semidilute polymer solutions for $T > T_{\text{gel}}$ and the work of Adam *et al.* and Martin, Wilcoxon, and Odinek below T_{gel} . Quantitatively, however, significant differences are found in the shape of the slower modes compared to earlier polymer work and the q dependencies of these modes compared to the gel

work. Because of this, we give an explanation of our observed phenomena based on anomalous diffusion [24] which describes our observations well. We then propose interpretation of this anomalous diffusion picture in terms of polymer molecule dynamics.

II. EXPERIMENTAL METHOD

Gelatin is a topologically linear random-coil molecule. It is perhaps the most well-known material to show gelation behavior being the basis for many foods and has been studied extensively in the past [25–27]. It is derived from naturally occurring collagen. The random coils are described by a fractal morphology with exponent determined by the nature of the intracoil screening. For modest concentrations these strands overlap, and when the temperature is lowered below $T_{\text{gel}} \approx 30^\circ\text{C}$, these regions of overlap nucleate to helix junctions. This junction-strand network grows to macroscopic size and a thermally reversible (i.e., “physical”) gel is formed.

In our work aqueous solutions of gelatin were made up by weight using distilled, deionized water and swine gelatin obtained from Aldrich. Once dissolved, the solutions were held at 45°C for one hour to remove any history-dependent effects. After such treatment, SDS gel filtration showed a monodisperse fraction with mole weight 1.2×10^5 amu. These hot solutions were then adjusted to other desired temperatures for further experimentation above the gel point or immediately quenched to a temperature less than the gel point temperature $T_{\text{gel}} \approx 30^\circ\text{C}$ in the light-scattering cell. This quench defined a quench time of zero, $t_q = 0$, and the systems were observed as a function of t_q . Gel times t_{gel} ranged from 100 to 250 min after $t_q = 0$ depending on temperature and concentration as determined by when the flow of a twin sample when gently tipped became nonsmooth or lumpy.

Dynamic light scattering was performed in the homodyne mode on ~ 5 ml of gelatin solution held in a thermostated ($\pm 0.1^\circ\text{C}$) cell to measure the scattered light intensity autocorrelation function $\langle I(0)I(t) \rangle$. An Ar^+ laser with $\lambda = 5145 \text{ \AA}$ and a commercial correlator with 64 channels were used [28]. Due to the breadth of the scattered light autocorrelation function, spectra were obtained at three or more different sample times typically spaced by a factor of 10 and then spliced together [28]. The autocorrelation function was used to calculate the background subtracted and normalized dynamic structure factor $S(q, t) = \{[\langle I(0)I(t) \rangle - B] / (\langle I^2 \rangle - B)\}^{1/2}$. The background B was determined from either the count statistics available in the correlator or the value of $\langle I(0)I(t) \rangle$ at sufficiently long t such that no more decay was observed. These values always agreed to better than 1%.

Solution viscosities were measured using a cone-and-plate viscometer at low shear rates such that the solution had Newtonian, i.e., shear-rate-independent behavior. This device was temperature controlled to $\pm 0.1^\circ\text{C}$.

III. RESULTS

Figure 1 displays examples of the dynamic structure factor $S(q, t)$ obtained from aqueous gelatin solutions for

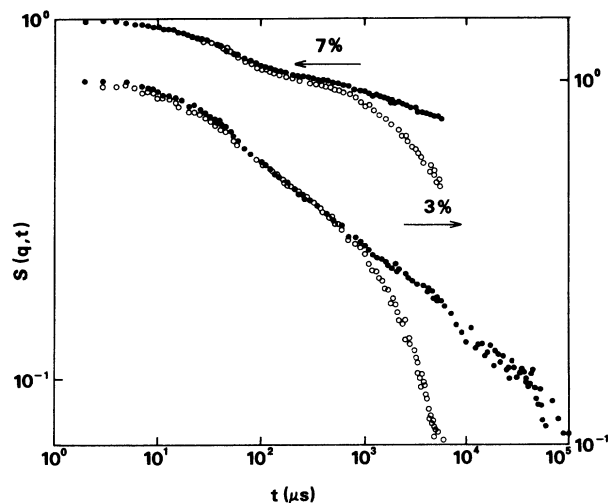


FIG. 1. Scattered light dynamic structure factor at $\theta = 90^\circ$ for 3% and 7.0% aqueous gelatin solutions for both $T = 45^\circ\text{C}$ (open circles) and $T = 27^\circ\text{C}$ (closed circles). When $T = 27^\circ\text{C}$ the systems had just evolved to a gel, i.e., $t_q = t_{\text{gel}}$.

both $T > T_{\text{gel}}$ and $T < T_{\text{gel}}$. Our analysis of the shape of these spectra yields three modes: a fast exponential decay at short times less than $\sim 50 \mu\text{sec}$ followed by a power-law decay which crosses over to a stretched exponential at long time. These decays may be fit in a piecewise manner to

$$S(q, t) \sim \begin{cases} e^{-D_f q^2 t}, & t \lesssim 50 \mu\text{sec} \\ t^{-\alpha}, & t < \tau_c \\ e^{-(t/\tau_c)^\beta}, & t \geq \tau_c \end{cases} \quad (1a) \quad (1b) \quad (1c)$$

In Eq. (1a) q is the scattering wave vector, $q = 4\pi n \lambda^{-1} \sin(\theta/2)$ where λ is the optical wavelength, n the sample index of refraction, and θ the scattering angle. The spectra for $T > T_{\text{gel}}$ were static, whereas for $T < T_{\text{gel}}$ the characteristic time τ_c evolved with t_q in a singular fashion as the solution set to a gel.

The fits to Eqs. (1) are demonstrated in Figs. 2–4. Figure 2 is a semilog graph of the initial decay part of the 3% gelatin, with $T = 27^\circ\text{C}$ data of Fig. 1. A straight line indicating a good exponential is seen.

Figure 3 is a double-log graph of a 3% solution that has been quenched from 45°C to 27°C . One can see that the region of power-law behavior, which is linear on such a graph, increases with time as the sol evolves to a gel. It would be easy to miss this power-law region in the initial semidilute polymer solution but the evolution with gelatin makes it apparent.

Figure 4 shows a semilog plot of $S(q, t)$ versus $(t/\tau_c)^\beta$ with $\beta = 0.67$ and $\tau_c = 6.21 \text{ msec}$ for the 3% gelatin at $T = 27^\circ\text{C}$ data in Fig. 1. Linearity for $(t/\tau_c)^\beta \geq 0.2$ indicates a stretched exponential with $\beta = 0.67$. We now consider these modes in turn in a more detailed manner.

Figure 5 shows the fast-mode diffusion coefficient D_f as a function of solution viscosity varied by changing the

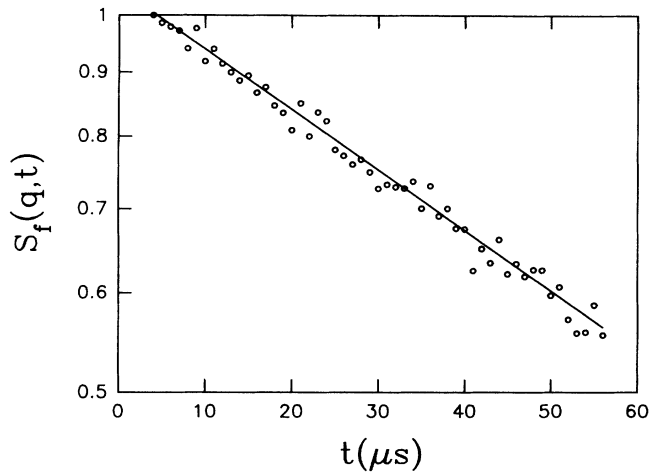


FIG. 2. Initial or fast decay of the dynamic structure factor for a 3% gelatin solution at $\theta=90^\circ$ for $T=27^\circ\text{C}$. The background was chosen as the value of the total structure factor (Fig. 1) at $t=120\ \mu\text{sec}$. Afterpulsing and electronic dead-time effects forced us to eliminate the first few μsec of the signal. Only the first 60 μsec are shown because beyond this the intermediate decay begins affecting the data.

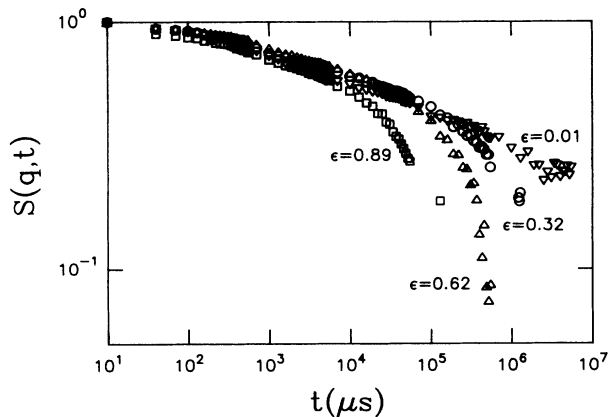


FIG. 3. Scattering light dynamic structure factor at $\theta=90^\circ$ for a 3.0% aqueous gelatin solution quenched to $T=27^\circ\text{C}$. The system evolved to a gel as a function of $\epsilon=(t_{\text{gel}}-t_q)t_{\text{gel}}^{-1}$.

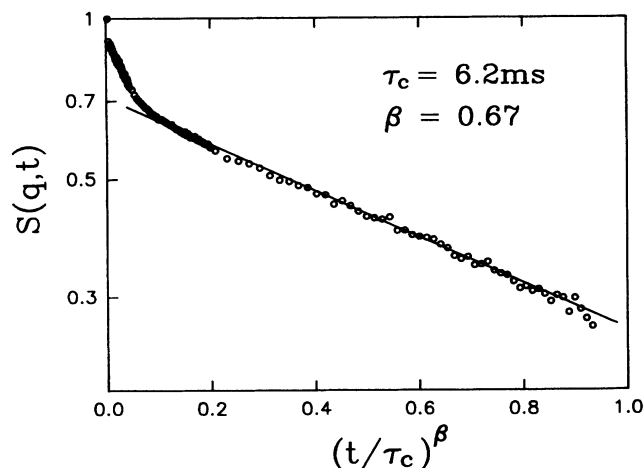


FIG. 4. The dynamic structure vs $(t/\tau_c)^\beta$ with $\beta=0.67$ for a 3% gelatin solution at $\theta=90^\circ$ and $T=27^\circ\text{C}$ far from the gel point with $\tau_c=6.2\ \text{msec}$.

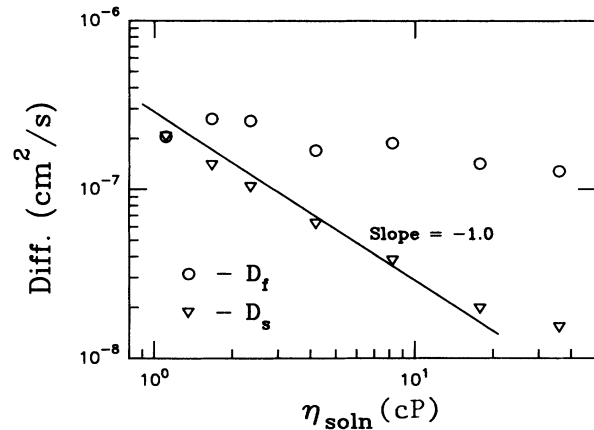


FIG. 5. Fast- and slow-mode diffusion coefficients D_f and D_s as a function of solution viscosity changed by changing the gelatin concentration at $t=45^\circ\text{C}$.

gelatin concentration at $T=45^\circ\text{C}$. Only a small dependency is seen, hence we conclude that D_f is not a function of the solution viscosity. On the other hand, we have found that D_f is a function of temperature in a manner which suggests it is inversely proportional to the solvent (water) viscosity η_{solv} . This is in agreement with Amis and co-workers [5] who also found that D_f was inversely proportional to the solvent viscosity. This implies a Stokes-Einstein relation, and an effective hydrodynamic size for the fast mode can be defined as

$$r_f = \frac{kT}{6\pi\eta_{\text{solv}}D_f} \quad (2)$$

Using $D_f=2\times 10^{-7}\ \text{cm}^2/\text{sec}$ and the viscosity of water at 45°C (0.596 cP), an effective size of 170 Å is obtained. This compares well to the radius of gyration of gelatin of 175 Å measured by static-light-scattering Zimm plots [29]. Amis and co-workers [5] measured a D_f for aqueous gelatin roughly a factor of 2 larger than our values. Their gelatin, however, had a smaller molecular weight of 35 000, hence we expect our D_f to be smaller.

The intermediate power-law-mode interpretation of the DLS spectrum is new to semidilute polymer solutions and was uncovered by the behavior of the solution as it set to a gel. In Fig. 6 we show $S(q, t)$ for a 3% aqueous gelatin solution near its gel point at three different scattering angles, hence q 's. A dependence of the slope of these graphs, hence α in Eq. (1b), is apparent. Values of α versus q are shown in Fig. 7. For both $T > T_{\text{gel}}$ and $T < T_{\text{gel}}$ the data display a linear dependence on this log-log plot with a slope of 2.0 to imply

$$\alpha = l_1^2 q^2 \quad (3)$$

Since α is unitless, the q dependence implies a new length scale l_1 .

We also found that α was concentration dependent. Thus l_1 is a function of the concentration c ; this is displayed in Fig. 8. The results are remarkable in that a scaling-type behavior is seen [1]. That is, l_1 is independent of c for $c \lesssim 3\%$ but develops an $l_1 \sim c^{-3/4}$ depen-

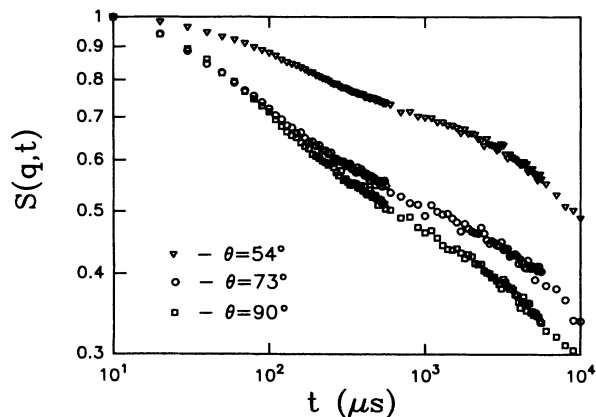


FIG. 6. The dynamic structure factor for 3% gelatin solution at 27°C near the gel point for three different scattering angles to show the q dependence of the intermediate mode.

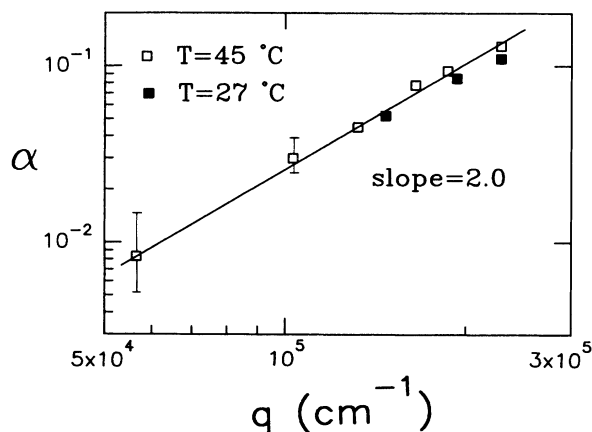


FIG. 7. The exponent α for the intermediate power-law part of the dynamic structure factor as a function of the scattering wave vector. Gelatin concentration was 3%.

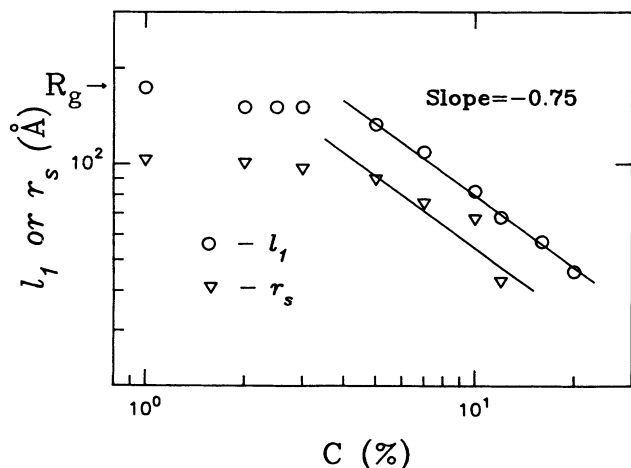


FIG. 8. Slow-mode hydrodynamic size r_s and intermediate mode length scale l_1 vs concentration.

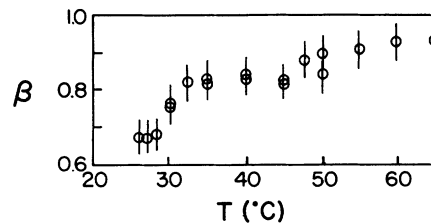


FIG. 9. The width exponent β for the stretched exponential part of the fit to the dynamic structure factor as a function of temperature.

dence for $c \gtrsim 3\%$. The polymer overlap concentration, as we have measured via intrinsic viscosity measurements, is $c^* \approx 2.5\%$. Furthermore, $l_1(c \rightarrow 0) = 170 \text{ Å}$ is in good agreement with the molecular radius of gyration $R_g = 175 \text{ Å}$ and our own measurement of $r_f = 170 \text{ Å}$.

The third or slowest decay also yields interesting empirical results. Figure 9 shows the width exponent β as a function of T . A rather sharp transformation occurs near 30°C, which is the gel temperature T_{gel} . Adam *et al.* [21] saw β decrease to $\sim \frac{1}{3}$ as polymer concentration increased; we do not see a concentration dependence. Martin, Wilcoxon, and Odinek [22,23] measured $\beta = 0.65$ in their gelling silica. This value agrees with our $\beta = 0.67 \pm 0.05$ in the gelling regime.

The characteristic time τ_c displays an interesting q dependence as shown in Fig. 10. In the sol at 45°C, $\tau_c \sim q^{-x}$ where $x = 2.5 \pm 0.2$. Thus we find both α and τ_c are both strongly dependent on q in the sol regime. This is in strong contrast to a significant amount of previous data on polymer solutions in which the slow mode, which we envision as an unresolved combination of our power-law and stretched exponential modes, is not q dependent. In Fig. 10 we also show data for $T < T_{\text{gel}}$ while the system is evolving to a gel. Here we roughly find $\tau_c \sim q^{-x}$ where $x = 3.0 \pm 0.4$ although there is considerable fluctuation in the data. Thus the q dependence of τ_c changes as we go across $T_{\text{gel}} \approx 30^\circ\text{C}$.

In Fig. 3 we saw how $S(q, t)$ evolved as the system

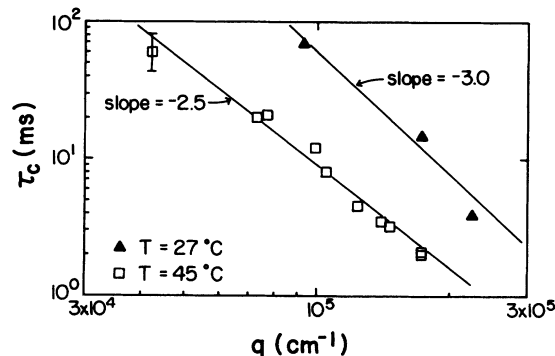


FIG. 10. The characteristic relaxation time τ_c vs the scattering wave vector for two different temperatures for the 3% gelatin solution. When $T = 27^\circ\text{C}$, τ_c diverges hence its value at $\epsilon = (t_{\text{gel}} - t_q)t_{\text{gel}}^{-1} = 0.8$ is shown as an example. A typical error bar is shown.

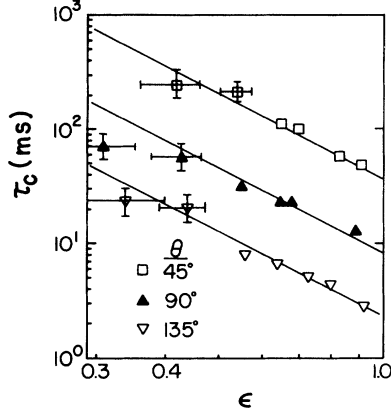


FIG. 11. The characteristic relaxation time τ_c vs $\epsilon = (t_{\text{gel}} - t_q)t_{\text{gel}}^{-1}$ for 3.0% aqueous gelatin at $T = 2.7^\circ\text{C}$ for three different scattering angles. Lines have slope -2.2 .

evolved from sol to gel. Essentially the only change was $\tau_c \rightarrow \infty$. Figure 11 shows the behavior of τ_c as the quenched system evolves to a gel as a function of the reduced gel times $\epsilon = (t_{\text{gel}} - t_q)t_{\text{gel}}^{-1}$. It appears that τ_c diverges as $\epsilon \rightarrow 0$ in a power-law fashion as

$$\tau_c \sim \epsilon^{-x} \quad (4)$$

with $x = 2.2 \pm 0.3$. Martin, Wilcoxon, and Odinek [22,23] saw a similar divergence with an exponent of 2.5 ± 0.1 . There appears to be some rounding in the proposed divergence below $\epsilon \sim 0.4$, possibly due to our uncertainty in the gel time t_{gel} .

IV. DISCUSSION

Our results indicate three modes of relaxation in semi-dilute polymer solutions: an exponential, followed by a power law, followed by a stretched exponential. Earlier work on polymer solutions saw an exponential followed by a broad slow mode, and we infer that this broad slow mode is, in gelatin at least, a combination of the power law and stretched exponential. As our system evolved from sol to gel, the stretched exponential characteristic time τ_c diverged to infinity or at least showed divergent behavior in the early stages of evolution. Power laws and stretched exponentials have been inferred in DLS data from at least two other gelling systems but the q dependencies, especially for the power law, appear to be significantly different.

What are the physical origins of the three modes of decay? We cannot at this time offer a final description. We can, however, offer a model based on anomalous diffusion [24] which reproduces the observed experimental facts for the second and third decays. After we present this model, we will become even more speculative and propose interpretations in terms of a microscopic picture of the polymer solution.

We interpret the fast exponential decay, as have previous workers [4–6], as the incipient gel mode due to short-range monomer or blob motion of the chains, and we discuss it no further here. For the second and third

decay we propose a mechanism based on anomalous diffusion [24], wherein the mean-squared displacements of the walkers are given by

$$\langle R^2 \rangle = \begin{cases} l_1^2 \ln(t/t_1), & t < \tau_c \\ 2l_2^2(t/t_2)^\beta, & t \geq \tau_c, \end{cases} \quad (5a)$$

$$(5b)$$

where the times t_1 and t_2 and the lengths l_1 and l_2 describe the elementary steps of the two random walks. Proposition (5a) is certainly *ad hoc*, having as yet no precedent or physical basis. However, simulations of random walks on fractal lattices [19] often qualitatively look like Eq. (5a) at early times. On the other hand, the form of proposition (5b) is known to occur for a random walk on a fractal lattice, and we shall make more of this below. To calculate the dynamic structure factor we use a Gaussian diffusion with a probability distribution $P(r,t) = (2\pi\langle R^2 \rangle)^{-1/2} \exp(-r^2/2\langle R^2 \rangle)$. $S(q,t)$ is the Fourier transform of $P(r,t)$ [30]. This assumption is an approximation in that numerical work on anomalous diffusion which leads to Eq. (5b) shows that the diffusion is non-Gaussian of the form $P(r,t) \sim \exp(-r^{2+\delta})$ [24]. Numerical evaluation of the Fourier transform of this with reasonable values of δ ($0 \leq \delta \leq 1$) show that the result obtained with the Gaussian assumption is a good approximation. We find the dynamic structure factor resulting from Eqs. (5) to be

$$S(q,t) \sim t^{-\alpha}, \quad \alpha = l_1^2 q^2; \quad t < \tau_c \quad (6a)$$

$$\sim e^{-(t/\tau_c)^\beta}, \quad \tau_c = (ql_2)^{-2/\beta} t_2; \quad t \geq \tau_c. \quad (6b)$$

This formulation incorporating anomalous diffusion successfully describes the form of $S(q,t)$ beyond the initial fast decay, Eq. (1), observed in our experiments. Furthermore, the correct q dependencies are obtained. For α , Eq. (6a) predicts the empirically determined Eq. (3) with the proper q dependence. For τ_c , Eq. (6b) predicts $\tau_c \sim q^{-2/\beta}$. From Fig. 9 when $T = 45^\circ\text{C}$, $\beta = 0.81 \pm 0.05$, hence $2/\beta = 2.47 \pm 0.16$ in good agreement with the experimental 2.5 ± 0.2 (Fig. 10). When $T = 27^\circ\text{C}$, $\beta = 0.67 \pm 0.05$, hence $2/\beta = 3.0 \pm 0.2$ in agreement with the experimental 3.2 ± 0.4 (Fig. 10).

For the third decay we may define a “slow-mode” diffusion coefficient as

$$D_s \equiv l_2^2/t_2 = t_2^{\beta-1} \tau_c^{-\beta} q^{-2}. \quad (7)$$

Note that D_s cannot be determined because t_2 is unknown. Despite this we can test the efficacy of this definition by studying the behavior of D_s with the solution viscosity. In Fig. 12 we plot a log-log graph of η_{soln}/T versus τ_c for a series of concentrations at different temperatures all above T_{gel} . For each concentration linearity with slope of 0.83 ± 0.05 is obtained. Since $\beta = 0.81 \pm 0.05$ (Fig. 9) for $T > T_{\text{gel}}$, this implies $T/\eta_{\text{soln}} \sim \tau_c^{-\beta}$. Thus, by Eq. (7), $D_s \sim T/\eta_{\text{soln}}$. This is in accord with the Stokes-Einstein equation $D = k_B T / 6\pi\eta_{\text{soln}}r$, and hence lends veracity to our definition of D_s in Eq. (7).

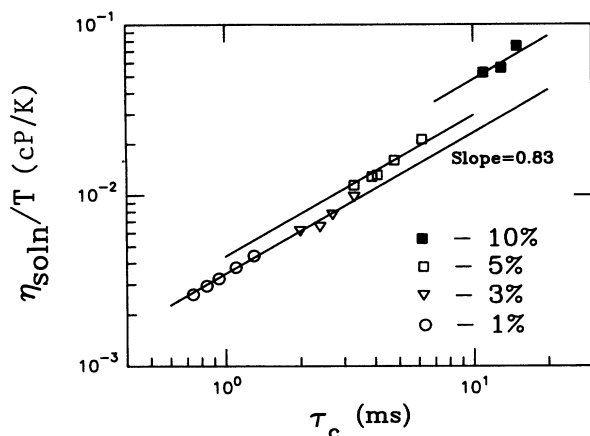


FIG. 12. Solution viscosity divided by temperature η_{soln}/T vs the characteristic relaxation time τ_c for solutions of various gelatin concentrations.

We return now to Fig. 5 where we have plotted D_s determined from the measured τ_c at various q and a t_2 value arbitrarily chosen so that $D_s = D_f$ at $c = 1\%$ near the limit of $c \rightarrow 0$. This t_2 value was $t_2 = 8.3 \times 10^{-10}$ sec. We see $D_s \sim 1/\eta_{\text{soln}}$ in contrast to D_f which has very little dependence.

Figure 13 plots D_s versus c , again using $t_2 = 8.3 \times 10^{-10}$ sec. For $c > c^* \approx 2.5\%$, $D_s \sim c^{-1.75}$, a behavior predicted by scaling [1]. Finally yet another permutation of the data can be obtained by defining a slow-mode hydrodynamic size via

$$r_s = k_B T / 6\pi\eta_{\text{soln}} D_s. \quad (8)$$

Figure 8 contains r_s versus c ; once again scaling behavior is seen.

We see that the anomalous diffusion model accurately predicts shape and q dependencies of $S(q, t)$. Furthermore various length scales and diffusion coefficients derivable from our data display reasonable scaling behavior with concentration with magnitudes in the $c \rightarrow 0$ limit equal to those expected from the size of the gelatin molecule. Thus a great deal of internal consistency is found in the data and the anomalous diffusion model. Now we at-

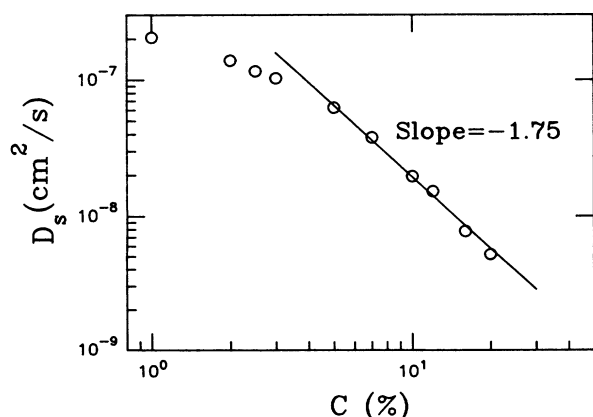


FIG. 13. Slow-mode diffusion coefficient vs concentration.

tempt to contend with the physical origins of our results. The following is quite speculative but is consistent with all our results and should be useful as a stepping stone for future refinement.

In the past [11–18] the fast and slow modes seen in DLS experiments on semidilute polymer solutions have been explained in terms of motion of the polymer which is topologically constrained to a tube along its length due to interaction with other polymers. For average displacements much less than the tube diameter a , the cooperative segmental motion gives rise to the fast mode, as mentioned above. We expect, however, that when the average displacement becomes comparable to a , the segmental motion toward the wall becomes severely hindered due to the constraints. Based on the $t^{-\alpha}$ behavior we observe for the second decay, we propose that this hindered motion is described by Eq. (5a). This is consistent with the identification of $l_1 = \xi$, the mesh size of the network which should display scaling behavior as seen in Fig. 8. As t approaches τ_c , which represents time for which reptation of the entire chain becomes significant, the average displacement perpendicular to the tube should approach the tube diameter a . Thus $\langle R^2(\tau_c) \rangle = l_1^2 \ln(\tau_c/t_1) \sim a^2$. Based on shear modulus measurements, it has been suggested that $a \sim c^{-1/2}$ for $c > c^*$ [31], where $c^* \approx 3\%$ is the overlap concentration. $R(\tau_c)$ is plotted in Fig. 14 and one sees consistency with this prediction for $c \gtrsim 8\%$.

The third mode occurs when $t \geq \tau_c$, and we ascribe it to full chain reptation along the tube. But why is the diffusion anomalous? Computer simulations have shown that a random walk on a fractal lattice is hindered relative to a complete Euclidean lattice due to the ramification of the possible sites the walker may occupy [24]. The evolution of the mean-square displacement is slower and behaves in the form given in Eq. (5b) with $\beta = d_s/d_f < 1$, where d_s is the spectral or fracton dimension and d_f is the fractal dimension of the lattice. It is found that very nearly $d_s = \frac{4}{3}$ [32]. Given this value of d_s , we need d_f to evaluate β and compare to our measurements. Agreement can be obtained if we use the fractal nature of single gelatin molecules and assume that below

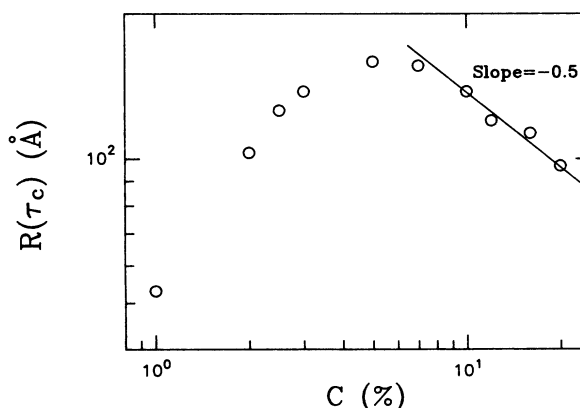


FIG. 14. Mean-square displacement of logarithmic diffusion, Eq. (5a), at τ_c vs concentration at $T = 45^\circ\text{C}$.

$T_{\text{gel}} \approx 30^\circ\text{C}$ water is a poor solvent for gelatin and hence the gelatin molecules are random chains with $d_f = 2$ [1]. Then $\beta = d_s/d_f = \frac{2}{3}$ in agreement with our data in Fig. 9. For $T > T_{\text{gel}}$ water becomes a better solvent, i.e., T_{gel} is near the theta temperature for gelatin in water, and the molecules are self-avoiding random chains with $d_f = \frac{5}{3}$. Then $\beta = d_s/d_f = \frac{4}{5}$, again in agreement with the data in Fig. 9 for $30^\circ\text{C} < T < 50^\circ\text{C}$. To explain why the polymer diffuses on a "lattice" of the same fractal dimension as the polymer, we need only recall the concept of reptation. That is, the tube in which the coil reptates should have, on large enough length scale, the same shape hence the same fractality of the coil. As the coil slithers along the tube, the head and tail move along the fractal path of the tube. It is the head and tail motion that contributes to the third, stretched exponential decay, the rest of the coil replacing itself along the length thus causing no index of refraction variation. Finally, τ_c diverges as the system sets to a gel. Gelation occurs due to random crosslinking of the polymer molecules. Thus the severely hindered motion region of Eq. (5a) becomes dominant as reptation becomes restricted.

V. CONCLUSION

In summary our dynamic-light-scattering measurements on aqueous gelatin solutions indicate three relaxations: an exponential at short times, followed by a power law at intermediate time, and a stretched exponential at long time. We interpret these modes as the normal "gel mode" due to cooperative segmental motion of the polymer, then anomalous diffusion where the mean-square displacement is proportional to $\ln t$ at intermediate time, and t^β with $\beta < 1$ at long time. Length scales derived from our model are consistent with molecular dimensions and scaling. The characteristic time dividing these regimes diverges as the system becomes a gel. The exponent $\beta = d_s/d_f$ where $d_s = \frac{4}{3}$ is the fracton density-of-states exponent and d_f is the fractal dimension of the individual gelatin molecules.

ACKNOWLEDGMENT

This work was supported by the Kansas State University Agricultural Experiment Station.

*Present address: Department of Basic Courses, Zhejiang Agricultural University, Hangzhou, Zhejiang, People's Republic of China.

†Present address: Physics Department, Huaqiao University, Quanzhou, Fujian, People's Republic of China.

- [1] P. G. DeGennes, *Scaling Concepts in Polymer Physics* (Cornell University Press, Ithaca, 1979).
- [2] M. Doi and S. F. Edwards, *The Theory of Polymer Dynamics* (Oxford University Press, Oxford, 1989).
- [3] D. W. Schaefer and C. C. Han, in *Dynamic Light Scattering*, edited by R. Pecora (Plenum, New York, 1985).
- [4] G. D. Patterson and G. C. Berry, *Studies Polymer Sci.* **2**, 73 (1987).
- [5] E. J. Amis, P. A. Janmey, J. D. Ferry, and H. Yu, *Macromolecules* **16**, 441 (1983).
- [6] E. J. Amis and C. C. Han, *Polymer* **23**, 1403 (1982); E. J. Amis, C. C. Han, and Y. Matsushita, *ibid.* **25**, 650 (1984).
- [7] E. J. Amis, C. C. Han, and Y. Matsushita, *Polymer* **25**, 650 (1984).
- [8] T. Chang and H. Yu, *Macromolecules* **17**, 115 (1984).
- [9] T. Tanaka, L. O. Hocker, and G. B. Benedek, *J. Chem. Phys.* **59**, 5151 (1973).
- [10] T. Tanaka, in *Dynamic Light Scattering* (Ref. [3]).
- [11] S. H. Kim, D. J. Ramsay, G. D. Patterson, and J. C. Selser, *Polym. Preprints* **28**, 363 (1987).
- [12] W. Burchard and M. Eisele, *Pure Appl. Chem.* **56**, 1379 (1984).
- [13] D. S. Cannell, P. Wiltzius, and D. W. Schaefer, in *Physics of Complex and Supramolecular Fluids*, edited by S. Safran and N. Clark (Wiley, New York, 1987), p. 267.
- [14] W. Brown, *Macromolecules* **19**, 1083 (1986).
- [15] T. Nicolai, W. Brown, R. M. Johnsen, and P. Stepanek, *Macromolecules* **23**, 1165 (1990).
- [16] T. Nicolai and W. Brown, *Macromolecules* **23**, 3150 (1990).
- [17] L. Fang and W. Brown, *Macromolecules* **23**, 3284 (1990).
- [18] T. Nicolai, W. Brown, S. Hvidt, and K. Heller, *Macromolecules* **23**, 5088 (1990).
- [19] D. Stauffer, *Introduction to Percolation Theory* (Taylor and Francis, London, 1985); *Phys. Rep.* **54**, 1 (1979).
- [20] D. Stauffer, A. Coniglio, and M. Adam, *Adv. Polym. Sci.* **44**, 103 (1962).
- [21] M. Adam, M. Delsanti, J. P. Munch, and D. Durand, *Phys. Rev. Lett.* **61**, 706 (1988).
- [22] J. E. Martin and J. P. Wilcoxon, *Phys. Rev. Lett.* **61**, 373 (1988).
- [23] J. E. Martin, J. P. Wilcoxon, and J. Odinek, *Phys. Rev. A* **43**, 858 (1991).
- [24] S. Havlin and D. Ben-Avraham, *Adv. Phys.* **36**, 695 (1987).
- [25] *The Science and Technology of Gelatin*, edited by A. G. Ward and A. Courts (Academic, New York, 1977).
- [26] M. Djabourov, J. Leblond, and P. Papon, *J. Phys. (Paris)* **44**, 319 (1988); **44**, 333 (1988).
- [27] M. Djabourov, *Contemp. Phys.* **29**, 273 (1988).
- [28] D. L. Sidebottom and C. M. Sorensen, *Phys. Rev. B* **40**, 461 (1989).
- [29] H. Boedtker and P. Doty, *J. Am. Chem. Soc.* **58**, 968 (1954).
- [30] B. J. Berne and R. Pecora, *Dynamic Light Scattering* (Wiley, New York, 1976).
- [31] W. W. Graessley, *Adv. Polym. Sci.* **16**, 1 (1974).
- [32] S. Alexander and R. Orbach, *J. Phys. (Paris) Lett.* **43**, L625 (1982).